Genome-Wide Screen for Context-Dependent Tumor Suppressors Identified Using in Vivo Models for Neoplasia in *Drosophila*

Casper Groth,*,† Pooja Vaid,* Aditi Khatpe,* Nelchi Prashali,* Avantika Ahiya,* Diana Andrejeva,†
Madhumita Chakladar,* Sanket Nagarkar,* Rachel Paul,* Devaki Kelkar,* Teresa Eichenlaub,†
Hector Herranz,† TS Sridhar,‡ Stephen M. Cohen,*,† and LS Shashidhara*,§,1

*Indian Institute of Science Education and Research (IISER) Pune, Dr. Homi Bhabha Road, Pashan, Pune 411008, India, †Department of Cellular and Molecular Medicine, University of Copenhagen, Blegdamsvej 3, Copenhagen 2200N, Denmark, ‡Division of Molecular Medicine, St Johns Research Institute, Bangalore, India, and §Department of Biology, Ashoka University, Sonipat, India

ORCID IDs: 0000-0001-5652-3351 (A.K.); 0000-0001-9306-1432 (L.S.)

ABSTRACT Genetic approaches in *Drosophila* have successfully identified many genes involved in regulation of growth control as well as genetic interactions relevant to the initiation and progression of cancer *in vivo*. Here, we report on large-scale RNAi-based screens to identify potential tumor suppressor genes that interact with known cancer-drivers: the Epidermal Growth Factor Receptor and the Hippo pathway transcriptional cofactor Yorkie. These screens were designed to identify genes whose depletion drove tissue expressing EGFR or Yki from a state of benign overgrowth into neoplastic transformation *in vivo*. We also report on an independent screen aimed to identify genes whose depletion suppressed formation of neoplastic tumors in an existing EGFR-dependent neoplasia model. Many of the positives identified here are known to be functional in growth control pathways. We also find a number of novel connections to Yki and EGFR driven tissue growth, mostly unique to one of the two. Thus, resources provided here would be useful to all researchers who study negative regulators of growth during development and cancer in the context of activated EGFR and/or Yki and positive regulators of growth in the context of activated EGFR. Resources reported here are available freely for anyone to use.

Studies in genetic models of tissue growth have identified networks of signaling pathways that cooperate to control growth during animal development (reviewed in (Harvey *et al.* 2013; Richardson and Portela 2017). Normal tissue growth involves controlling the rates of cell proliferation and cell death, as well as cell size, cell shape, etc. Signaling pathways mediate hormonal and neuroendocrine regulation of growth, which depend on nutritional status. Cell interactions also contribute to coordinating growth of cells within a tissue.

Growth regulatory pathways include both positive and negative elements to allow for feedback regulation. These feedback systems confer robustness to deal with intrinsic biological noise, and with a fluctuating external environment (Herranz and Cohen 2010). They also provide the means for different regulatory pathways to interact (Ren *et al.* 2010; Herranz *et al.* 2012a; Reddy and Irvine 2013). In the context of tumor formation, this robustness is reflected in the difficulty in generating significant misregulation of growth - a twofold change in expression of many growth regulators seldom has a substantial effect on tissue size in *Drosophila* genetic models. More striking is the difficulty in transitioning from benign overgrowth to neoplasia: hyperplasia does not normally lead to neoplasia without additional genetic alterations (*e.g.*, (Huang *et al.* 2005; Herranz *et al.* 2012b 2014).

Cancers typically show mis-regulation of multiple growth regulatory pathways. Mutational changes and changes in gene expression status contribute to driving cell proliferation, overcoming cell death and cellular senescence, as well as to allowing cells to evade the

checkpoints that normally serve to eliminate aberrant cells. These changes alter the normal balance of cellular regulatory mechanisms, from initial cellular transformation through disease progression (Stratton 2011; Alexandrov *et al.* 2013). For many tumor types, specific mutations have been identified as potent cancer drivers, with well-defined roles in disease (Kandoth *et al.* 2013; Zehir *et al.* 2017). However, most human tumors carry hundreds of mutations, whose functional relevance is unknown. The spectrum of mutation varies from patient to patient, and also within different parts of the same tumor (McGranahan and Swanton 2017). Evidence is emerging that some of these genetic variants can cooperate with known cancer drivers during cellular transformation or disease progression. The mutational landscape of an individual tumor is likely to contain conditional oncogenes or tumor suppressors that modulate important cellular regulatory networks.

Sequence-based approaches used to identify cancer genes favor those with large individual effects that stand out from the 'background noise' of the mutational landscape in individual cancers (Stratton 2011; Alexandrov *et al.* 2013). *In vivo* experimental approaches are needed to assign function to candidate cancer genes identified by tumor genome sequencing, and to identify functionally significant contributions of genes that have not attracted notice in genomics studies due to low mutational frequency, or due to changes in activity not associated with mutation. *In vivo* functional screens using transposon mutagenesis of the mouse genome have begun to identify mutations that cooperate with known cancer driver mutations, such as K-Ras, in specific tumor models (Copeland and Jenkins 2010; Pérez-Mancera *et al.* 2012; Takeda *et al.* 2015). Genetic approaches using *Drosophila* models of oncogene cooperation have also been used to identify genes that act together with known cancer drivers in tumor formation (Brumby and Richardson 2003; Pagliarini and Xu 2003; Wu *et al.* 2010; Brumby *et al.* 2011; Herranz *et al.* 2012b 2014; Eichenlaub *et al.* 2016; Richardson and Portela 2017; Song *et al.* 2017). The simplicity of the *Drosophila* genome, coupled with the ease of large-scale genetic screens and the high degree of conservation of major signaling pathways with humans, make *Drosophila* an interesting model to identify novel cancer genes and to study the cellular and molecular mechanisms that underlie tumor formation *in vivo* (reviewed in (Gonzalez 2013; Herranz *et al.* 2016; Sonoshita and Cagan 2017; Richardson and Portela 2018).

In *Drosophila*, overexpression of the Epidermal Growth Factor Receptor, EGFR, or Yorkie (Yki, the fly ortholog of the YAP oncoprotein) cause benign tissue over-growth (Huang *et al.* 2005; Herranz *et al.* 2012a 2014). Combining these with additional genetic alterations can lead to neoplastic transformation and eventually metastasis (Herranz *et al.* 2012b 2014; Eichenlaub *et al.* 2016, 2018; Song *et al.* 2017). Here, we report results of large-scale screens combining UAS-RNAi transgenes with EGFR or Yki expression to identify negative regulators of these growth regulatory networks that can lead to aggressive tumor formation *in vivo*. We also performed an independent screen to identify factors that could suppress EGFR-driven neoplasia. These screens have identified an expanded genomic repertoire of potential tumor suppressors that cooperate with EGFR or Yki. We have also identified few positive regulators of growth in the context of activated EGFR. Interestingly, there was limited overlap among the genes that cooperated with EGFR and those that cooperated with Yki. Gene intractome analysis and analyses of cancer databases for human orthologs of positives of these screens suggest that a large number of them have strong correlations to many clinical parameters. The output of this screen would, therefore, be useful to all researchers who study negative regulators of growth during development and cancer in the context of activated EGFR and/or Yki. Resources reported here are freely available for anyone to use.

MATERIALS AND METHODS

RNAi Screens

The KK transgenic RNAi stock library was obtained from the Vienna *Drosophila* RNAi Center (www.vdrc.at; also listed in Table S1) carrying inducible UAS-RNAi constructs on Chromosome II. For each cross, 5 males from the KK transgenic RNAi stock were crossed separately to 10-15 virgins from each of the following three driver stocks (see Supplemental Fig. S1A for the schematics of fly stocks): w*; ap-Gal4, UAS-GFP/CyO; UAS-Yki, tub-Gal80^{ts}/TM6B (Yki driver; Song *et al.* 2017); w*; ap-Gal4, UAS-GFP/CyO; UAS-EGFR, tub-Gal80^{ts}/TM6B (EGFR driver; Herranz *et al.* 2012b); and w*; ap-Gal4, UAS-GFP/CyO; and w*; ap-Gal4, UAS-GFP, Socs36E^{RNAi}/CyO; UAS-EGFR, tub-Gal80^{ts}/TM6B (EGFR driver +SOCS36E^{RNAi}). The combination of UAS-EGFR and UAS- SOCS36E^{RNAi} inducing tumorous growth is reported in Herranz *et al.* (2012b).

Virgin female flies were collected over 4-5 days and stored at 18° in temperature-controlled incubators on medium supplemented with dry yeast, prior to setting up crosses. Virgin females were mated to KK stock males (day 1) and the crosses were stored at 18° for 4 days to provide ample time for mating before starting the timed rearing protocol used for the screen. On day 5, the crosses were transferred into new, freshly yeasted vials for another 3 days at 18°. On day 8, the adult flies were discarded, and larvae were allowed to develop until day 11, at which time the vials were moved to 29° incubators to induce Gal4 driver activity. Crosses were aged at 29° for a further 8-9 days, after which larvae were scored for size and wing disc overgrowth phenotypes for Yki and EGFR driver screen crosses. Flies were scored for suppression of the tumor phenotype for the EGFR driver +SOCS36E^{RNAi} crosses (see Supplemental Fig. S1B for the screen workflow).

In order to verify the integrity of the driver stocks during the course of the screen, we examined their expression patterns in conjunction with setting up screen crosses each week. For each driver, 2-3 of the bottles used for virgin collection were induced at 29° for 24 hr and analyzed using fluorescence microscopy for apterous-Gal4 specific expression in wandering 3-instar larvae (see Supplemental Fig. S2 for larval images of quality control). Any batch that showed tumorous growth on its own without a cross with KK-RNAi line (in case of SOCS stocks, if the batch didn't show tumorous growth) were discarded and new batches were made from the original clean stock.

Positive hits form the initial screen were retested by setting up 2 or more additional crosses. The hits were scored as verified if 2 out of 3 tests scored positive. Wandering third instar larvae of confirmed positives were imaged and documented using fluorescence microscopy.

Genomic DNA PCR 40D landing site occupancy test

Genomic DNA from a select number of *Drosophila* KK transgenic RNAi library stocks was isolated following a protocol available at the VDRC (www.vdrc.at). The presence or absence of the KK RNAi transgene at the 40D insertion site on the second chromosome was determined by multiplex PCR using the following primers:

40D primer (C_Genomic_F): 5′-GCCCACTGTCAGCTCTCAAC-3′
pKC26_R: 5′-TGTAAAACGACGGCCAGT-3′
pKC43_R: 5′-TCGCTCGTTGCAGAATAGTCC-3′

PCR amplification was performed using GoTaq G2 Hot Start Green Master Mix kit (Promega) in a 25 μL standard reaction mix

and the following program: initial denaturation at 95° for 2 min, followed by 33 cycles with denaturation at 95° for 15 sec, annealing at 58° for 15 sec and extension at 72° for 90 sec. One final extension reaction was carried out at 72° for 10 min. Reactions were stored at -20° prior to gel loading. PCR using these primers generate an approximately 450 bp product in case of a transgene insertion or a 1050 bp product in case of no transgene insertion site at 40D.

Screen database
Results from the three screening projects were added to a screen management database, http://www.iiserpune.ac.in/rnai/, including images of positive hits and background information such as RNAi line ID, corresponding gene information from the Flybase etc. The database was developed by Livetek Software Consultant Services (Pune, Maharashtra, INDIA).

Pathway and gene set enrichment analysis
Gene set enrichment analysis was performed using genes that upon down regulation induced tumor formation (EGFR, YKI background) or suppressed tumor formation (EGFR+SOCS background). For *D. melanogaster* enrichment analysis all *D. melanogaster* protein coding genes were used as the "gene universe" together with organism specific datasets. For human ortholog enrichment analysis all human protein coding genes were used as the "gene universe" together with organism specific datasets. The algorithm packages and databases used in analysis are listed in Supplemental Tables S2 and S3. Unless otherwise specified, pathway databases included in these packages were used. The KEGG database was downloaded directly from source on 10.10.2018. Organ system specific and disease related pathway maps were excluded from this analysis. Minimum and maximum number of genes per pathway or gene set, significant criteria, minimum enriched gene count and annotated gene counts for each test and database are indicated in Supplemental Tables S2 and S3. GO results were filtered for level >2, to eliminate broad high-level categories and <10 to minimize duplication among subcategories. A representative term was selected in the cases were identical set of genes mapped to multiple terms within the same database. After filtering, the top 10 terms from each database were used for clustering analysis.

Pathway and gene set enrichment analysis results were visualized as enrichment map with appropriate layout based on gene overlap ration using igraph. Gene overlap ratio was set as edge width. Edges with low overlap were deleted, filtering threshold was based on a number of "terms" in the results table – from 0 to 50 by 10; increasing filtering thresholds from 0.16 to 0.26 by 0.2. Clusters were detected using "Edge betweenness community" algorithm. Similar biological processes were color-coded.

R packages
clusterProfiler (3.8.1) - (Yu *et al.* 2012).

ReactomePA (1.24.0) - (Yu and He 2016).

http://pubs.rsc.org/en/Content/ArticleLanding/2015/MB/C5MB00663E.

graphite (1.26.1) - Sales G, Calura E, Romualdi C (2018). graphite: GRAPH Interaction from pathway Topological Environment. R package version 1.26.1.

igraph (1.2.2) - Csardi G, Nepusz T: The igraph software package for complex network research, InterJournal, Complex Systems 1695. 2006. http://igraph.org

Database references
KEGG – (Kanehisa *et al.* 2016, 2017).

REACTOME – (Fabregat *et al.* 2018)

Panther – (Thomas *et al.* 2003)

GO – (Ashburner *et al.* 2000).

STRING interaction maps
STRING v10 is a computational tool for protein interaction network and pathway analysis (Szklarczyk *et al.* 2017)), to identify significant functional clustering among the candidate genes. STRING builds interaction maps by combining experimental data (including protein interaction data) with information about functional associations from text mining. STRING interactome maps were used to search for statistically significant enrichment of KEGG pathways.

Data availability
All stocks are available on request. Supplement Table S1 provides details of all RNAi lines used and link to the corresponding genes in the Flybase. Complete screen information along with larval images of the positives is also accessible from: http://www.iiserpune.ac.in/rnai/. Supplemental material available at figshare: https://doi.org/10.25387/g3.12746513.

RESULTS
Overexpression of EGFR or Yki proteins in the *Drosophila* wing imaginal disc produces tissue overgrowth. Under these conditions the imaginal discs retain normal epithelial organization, but grow considerably larger than normal. However, in combination with additional genetic or environmental changes, the tissue can become neoplastic and form malignant tumors (Herranz *et al.* 2012b 2014; Song *et al.* 2017; Eichenlaub *et al.* 2018). In this context, we carried out large-scale screens using UAS-RNAi lines from the Vienna *Drosophila* RNAi KK library to identify genes which would drive hyperplastic growth to neoplastic transformation when down-regulated. To facilitate screening for tumorous growth, we expressed UAS-GFP with UAS-EGFR or UAS-Yki to allow imaginal disc size to be scored in the intact 3rd instar larva (Figure 1A; screen design, examples and quality controls are shown in Supplemental Figures S1 and S2).

A large panel of independent UAS-RNAi lines were tested for their effects on tissue growth in the EGFR and Yki expression backgrounds (Figure 1B). Of ~8800 lines tested (Table S1), 74 interacted with EGFR to produce tumors (~1%), whereas 904 interacted with Yki (~10%) (Table S2). There was limited overlap, with only 21 RNAi lines producing tumors in both screens (Figure 1B), but we note that some loci that would be expected to score as hits in both screens, such as *dlg*, *scrib* and *l(2)gl*, were not targeted by RNAi lines in the KK collection, and so were not tested. In a parallel screen, we started with neoplastic tumors produced by co-expression of UAS-EGFR and UAS-SOCS36E[RNAi] [Herranz *et al.* 2012] and asked whether including expression of another RNAi transgene could suppress neoplasia (Figure 1A, right panels). SOCS36E depletion has been reported to potentiate EGFR driven tumor formation by alleviating repression of JAK Stat activity [8]. Of ~8900 lines tested (listed in Supplemental Table S1), 32 suppressed tumor formation in this assay (Figure 1B). Supplemental Table S2 (A) lists the genes identified in these three screens. In previous studies, massive disc overgrowth as in Figure 1(A) was often associated with loss of apically localized Actin and E-Cadherin: features indicative of Epithelial Mesenchymal Transition (EMT); and with formation of malignant
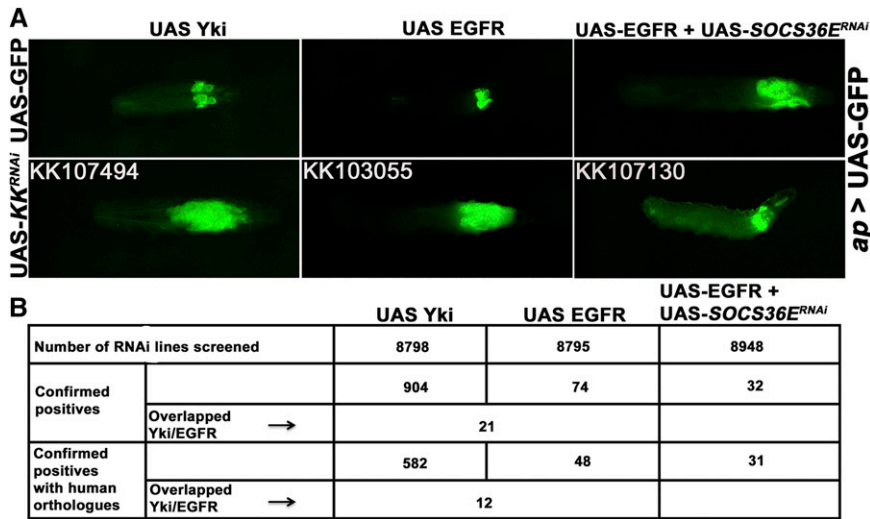
Figure 1 tumor formation/suppression visualized in intact larvae (A) Larvae co-expressed UAS-GFP with the indicated transgenes to permit visualization of the imaginal discs in the intact animal. All samples carried the ap-Gal4 driver and UAS-GFP. In addition, they carried either a second copy of UAS-GFP or one of the following: UAS-Yki, UAS-EGFR or UAS-EGFR+UAS-SOCS36E^{RNAi}. (B) Table summarizing the number of RNAi lines screened and identified in the three large-scale screens (represents those many number of interacting genes).

B

		UAS Yki	UAS EGFR	UAS-EGFR + UAS-SOCS36E^{RNAi}
Number of RNAi lines screened		8798	8795	8948
Confirmed positives		904	74	32
	Overlapped Yki/EGFR →	21		
Confirmed positives with human orthologues		582	48	31
	Overlapped Yki/EGFR →	12		

transplantable tumors [Herranz *et al.* 2012b, 2014; Song *et al.* 2017). Apico-basal polarity and Matrix Metalloprotease 1 (MMP1) expression were assessed for a randomly selected subset of lines from the EGFR and Yki screens to assess neoplastic transformation (Figure S3).

To identify the processes and pathways responsible for the interaction with the screen drivers, we looked for over-representation of biological functions among the screen positives using gene set enrichment analysis and the KEGG, REACTOME, GO and PAN-THER databases. Figure 2 presents the results of the enrichment analysis as graphical interaction maps, with similar biological processes color-coded. Edge length represents similarity between genes associated with significantly enriched terms. Thus, similar terms are closer together and form a community of biological process. The genes in each cluster are shown in Figure 2 and listed in Supplemental Table S3.

Genes that potentially modulate EGFR function during growth control

For discs overexpressing EGFR, we observed enrichment of RNAi lines targeting the Hippo pathway, growth signaling, and apoptosis (Figure 2A, B). Many of the genes in the Hippo pathway act as negative regulators of tissue growth, so their depletion by RNAi is expected to promote growth. The Hippo pathway is known to interact with the EGFR pathway to regulate normal developmental growth (Ren *et al.* 2010; Herranz *et al.* 2012a; Reddy and Irvine 2013). The Hippo pathway hits included core elements of the pathway, *hpo*, *wts* and *mats*, which serve as negative growth regulators; the upstream pathway regulators fat (an atypical cadherin) and expanded; as well as the transcriptional corepressor grunge, which is linked to Hippo pathway activity (Table S3). Several of these loci also contributed to the enrichment of terms linked to apoptosis, along with *pten*, a phospholipase that serves as a negative regulator of PI3K/AKT signaling, protein kinase A-C1, Src42A, the insulin-like peptide, ilp4, which are also linked to growth control (Table S3).

For suppression of tumors in discs overexpressing EGFR together with SOCS36E RNAi, we observed enrichment of RNAi lines targeting signaling pathways related to growth, including elements of the AKT/PI3K pathway (Figure 2E, F, Table S3). These pathways may be required for neoplasia in this EGFR driven tumor model. Interestingly, this pathway was also identified in a screen for synthetic lethals interacting with RasV12 (Willecke *et al.* 2011). As would be expected, depletion of Egfr limited tumor growth. Also enriched was a set of

genes involved in protein synthesis (Table S3). This may reflect a need for active cellular growth machinery to support tumor growth. The significance of genes involved in RNA splicing merits further investigation.

Genes that potentially modulate Yki function during growth control

For discs overexpressing Yki, RNAi lines targeting the Hippo pathway and associated growth regulators led to tumor production (Figure 2C, D, Table S3). These include *hpo*, *sav*, *wts*, *mats*, *ft* and *Grunge* (*Gug*). Although *wts* null mutants show some loss of neuronal differentiation and impairment of polarity (Menut *et al.* 2007) tumor formation solely due to elevated Yki activity has not been observed previously in *Drosophila*. It is worth noting that overexpression of YAP has been shown to lead to neoplasia in mouse liver and intestinal epithelial models (Dong *et al.* 2007; Cai *et al.* 2010). While most cancers appear to result from activation/inactivation of multiple genes and pathways, sufficient activation of the Yki or Yap can result in neoplasia.

The Hippo tumor suppressor pathway is regulated by cell polarity, cell contact, and mechanical forces (Wada *et al.* 2011; Halder *et al.* 2012; Aragona *et al.* 2013) as well as by other growth signaling pathways. The atypical Cadherin Fat mediates cell interactions and acts upstream of the Hippo pathway. Gug is the fly ortholog of the mammalian Atrophin/RERE proteins, and has been reported to interact physically and genetically with Fat (Fanto *et al.* 2003). Growth signaling pathways involving the *sgg*, *pten*, PKA-C1, TSC1 genes among others, were also identified. Additionally, a number of genes linked to membrane-cytoskeleton interaction and transmembrane transport were found to interact, including Arf and Rab family members. We also noted the enrichment of terms related to lipid and general metabolism. Regulation of lipid metabolism might affect the properties of cellular membranes. An intriguing subgroup contain genes related to glutamatergic signaling, including the vesicular glutamate transporter VGlut and the Eaat plasma membrane glutamate transporters. This finding is of interest in light of the results of an *in vivo* chemical screen which showed that that scribble mutant RasV12 tumors are glutamine-dependent (Willoughby *et al.* 2013). These tumors upregulate Yki and require Yki for tumor growth (Doggett *et al.* 2011).

Another major finding from this screen is the fact that many components of the machinery causing Promoter proximal pausing of
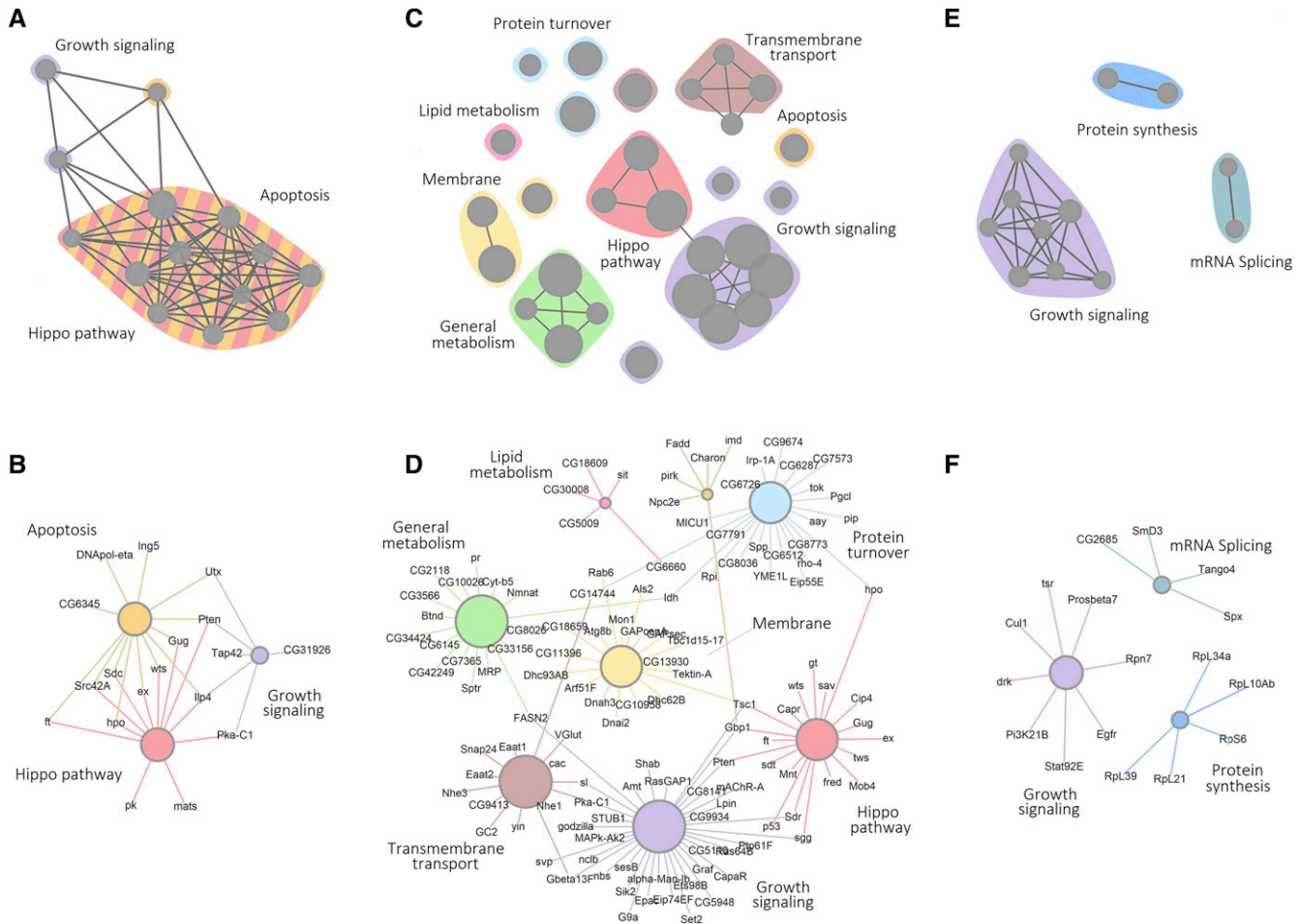
Figure 2 Summary of pathway enrichment analysis of fly genes identify in the *in vivo* screens reported here. (A, C, E) The results of the pathway and gene set enrichment analysis are shown as graphical interaction maps. Each node represents a significantly enriched term or pathway from the GO, KEGG, Reactome and Panther databases (Table S3). Color-coding indicates functionally related groups of terms. Lines indicate genes shared among different terms. (B, D, F) show the individual genes associated with functionally enriched cluster. (A, B) UAS-EGFR screen (C, D) UAS-Yki screen (E, F) UAS-EGFR+UAS-SOCS36E[RNAi] screen

RNA Polymerase II (such as components of the 7SK snRNAP and NELF complexes) are when depleted, enhanced Yki-driven growth leading to neoplastic transformation of *Drosophila* wing imaginal discs (Nagarkar *et al.* 2020). Additional work suggested that this phenomenon is dependent on CDK9 function and also specific to Yki-induced growth context (Nagarkar *et al.* 2020).

The large number of Yki interactors could reflect greater sensitivity of the screen. Alternatively, it might indicate a high false positive rate. While this screen was in progress, Vissers *et al.* (Vissers *et al.* 2016), reported that some of the RNAi lines from the Vienna *Drosophila* RNAi KK library have the potential to produce false positives in screens based on sensitized Hippo pathway phenotypes. This proved to be due to the presence of a second transgene landing site at 40D that was found in a subset of KK lines, in addition to the 30B landing site (Green *et al.* 2014; Vissers *et al.* 2016). We tested the 40D landing site strain (Vissers *et al.* 2016) and found that it did not cause a tumor phenotype under the conditions used for the screen. Nonetheless, we sampled the 40D status for a large subset of our Yki interactors (Table S2, 734/904) and found that 45% of them had insertions at 40D. A small survey comparing KK lines with Trip and GD lines showed that 65% of genes for which the KK line had a 40D site retested positive for interaction with Yki using an independent

(non-KK) transgene (15/23). The Yki-interaction screen should therefore be viewed as a more sensitized sampling of potential interactors, compared to the EGFR-interaction screen.

STRING interactome analyses

To view all genes identified in the three screens as one functional unit (for the fact that they were all growth regulators in one or the other contexts), we made use of STRING v10 (Szklarczyk *et al.* 2017) to produce protein interaction maps. STRING v10 builds interaction maps by combining experimental data (including protein interaction data) with information about functional associations from text mining. STRING v10 also uses information of co-occurrence, co-expression, gene neighborhood, gene fusion, and does sequence similarity search to predict functional interaction between proteins. An interaction pair supported by multiple lines of evidence has higher confidence score than other pairs.

Figure 3A shows the STRING interaction map for the genes identified as interactors of EGFR. As noted above, Hippo pathway (red) components were prominent among the genes identified as cooperating with EGFR to drive tumor formation. Figure 3(B) shows the interaction map for the genes identified as interactors of Yki. The larger number of hits in this screen results in a more complex
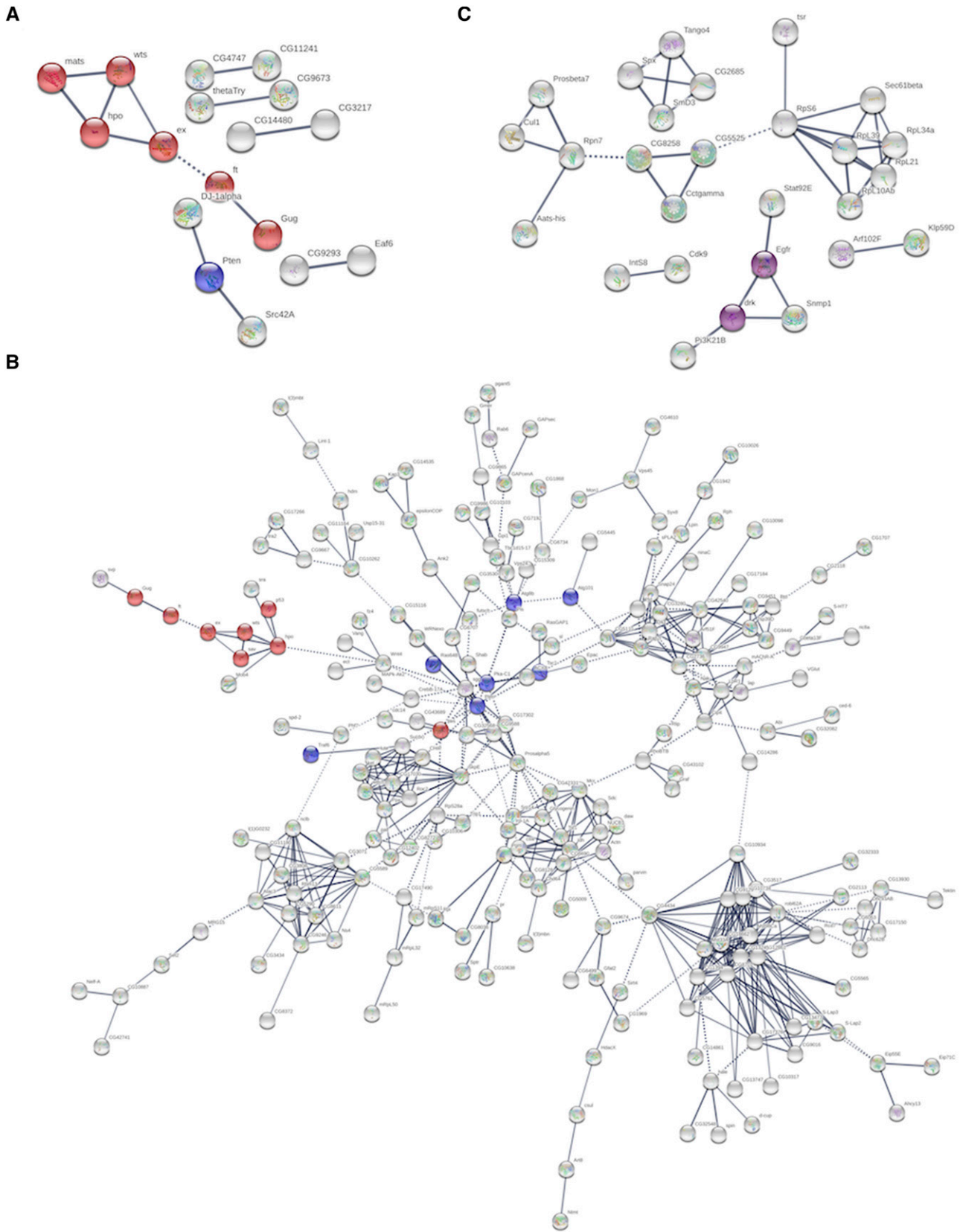
Figure 3 STRING interactome analysis of potential interactors of EGFR and YKi in *Drosophila*. STRING analysis was performed with confidence score of 0.7 and MCL clustering value of 2. (A) STRING Interactome of 73 fly genes identified as potential negative regulators in the context of over expression of EGFR. 17 out of those formed molecular clusters (with PPI enrichment value of 0.000482), largest being a cluster of 6 genes, all of which are constitutes of Fat/Hippo pathway (shown in red; FDR-1.39E^{-5}). (B) STRING Interactome of 888 genes of identified as potential negative

interaction map, with multiple interconnected clusters. The Hippo pathway (red) was again prominent in the fly screen. We also noted clusters containing elements of the ubiquitin mediated proteolysis pathway (green) and the PI3K/TOR (blue). As noted above, the higher sensitivity of this screen leads to the inclusion of weaker interactors, which may add to the complexity of these interaction maps. A focus on the stronger clusters and the interaction between them should guide future studies. Figure 3(C) shows interaction map for the genes identified as interactors of EGFR in the suppressor screen (in discs overexpressing EGFR together with SOCS36E RNAi). Among fly genes, as expected, we observed suppression of the tumor phenotype when components of EGFR pathway are down regulated.

Human orthologs of the fly genes identified in the three screens

To identify human orthologs for the candidate genes, we used the DRSC Integrative Ortholog Prediction Tool, DIOPT (Version 7.1, March 2018; www.flybase.org). DIOPT scores reflect the number of independent prediction tools that identify an ortholog for a given *Drosophila* gene. Orthology relationships are usually unambiguous when found by most of the 12 independent prediction tools in DIOPT. Table S2 lists the primary human orthologs (highest weighted DIOPT score), as well as the other orthologs with a weighted DIOPT score >2 for each of the hits in the fly screen. The primary human ortholog was used for subsequent analysis. In cases where multiple human orthologs had the same score, all orthologs with highest weighted DIOPT score were used. Out of 73 EGFR positive hits, 46 genes had one or more human orthologs, in total mapping to 50 human genes. Out of 32 SOCS positive hits 30 genes had one or more human orthologs, in total mapping to 31 human genes. Out of 904 YAP positive hits 570 genes had one or more human orthologs, in total mapping to 611 human genes.

To view the human orthologs in a functional context, we performed a gene set enrichment analysis and the KEGG, REACTOME, GO, PANTHER, NCI, MsigDB, BIOCARTA databases. Figure 4 presents the results of the enrichment analyses as graphical interaction maps, with similar biological processes color-coded. Edge length represents similarity between genes associated with significantly enriched terms. Thus, similar terms are closer together and form a community of biological processes. The genes in each cluster are shown in Figure 4 and listed in Supplemental Table S4. Because the enrichment analysis is highly sensitive to the number of orthologs for each of the fly genes, we used the minimal set consisting of only the primary human orthologs.

Hippo pathway components were enriched among the orthologs cooperating with EGFR to drive tumor formation (Figure 4A, B; Table S3). Two of these, LATS1 and STK3, also contributed to enrichment for a term linked to protein turnover. Regulation of protein turnover is an important mechanism for controlling the activity of a number of Hippo pathway components. For the screen for suppression of tumors in discs overexpressing EGFR together with SOCS36E RNAi, we observed enrichment of orthologs targeting growth signaling pathways, protein synthesis and mRNA splicing (Figure 4E, F, Table S4), similar to what was seen for the fly gene set

analysis. We also observed enrichment of pathways related to protein folding and molecular chaperones, in the human gene set. For the Yki screen, the human ortholog set was enriched for terms related to general metabolism, and membrane transport, as well as growth signaling, and other signaling pathways, including genes involved in protein turnover (Figure 4C, D).

METABRIC Analysis

We also studied gene expression levels in cancer patients by systematically querying METABRIC (Pereira *et al.* 2016) a large database on breast cancer. We chose this as breast cancer is an epithelial cancer and the distribution of treatment-naïve samples from very early to late stages are well characterized. More importantly, gene expression patterns have been well studied at genomic level for all stages of the cancer. For each of the human orthologs of the genes identified in the Yki screen, we examined how their expression levels (low levels, median levels and high levels) are correlated to clinical parameters/attributes such as months of disease-free survival, early *vs.* old age of the patients at diagnosis, Lymph node status at diagnosis, tumor grade III or above at diagnosis, early *vs.* late stages of cancer at diagnosis and small *vs.* large tumors at diagnosis. Total 365 human orthologs showed significant correlation to disease-free survival. Among them 186 were associated with their low levels of expression and 179 with high levels of expression (see Supplement Table S4 and Supplemental_Information_METABRIC analysis). The fact that higher levels of expression correlate to aggressive tumors suggest that they are potential growth promoters, while their fly homologs were identified as potential tumor suppressors in our screen. This discrepancy could be due to more complex nature of growth control in human, wherein a conserved pathway may have different outcomes in different contexts. Expression levels of 76 genes also showed strong correlations to the three clinical parameters as listed above (see Supplement Table S4 and Supplemental_Information_METABRIC analysis) indicating their critical role in growth control and impairment in their expression causing tumorous growth. Taken together, the positive hits in these screens would be useful for studies on growth control in development model organisms and in the context of cancer in human.

DISCUSSION

The Hippo pathway has emerged from this study as the single most important pathway limiting tumor formation in *Drosophila*. Increasing Yki activity by depletion of upstream negative regulators promoted tumor formation in both the EGFR and Yki hyperplasia models. Yki controls tissue growth by promoting cell proliferation and by concurrently inhibiting cell death through targets including Diap1, cycE and bantam miRNA (Tapon *et al.* 2002; Huang *et al.* 2005; Nolo *et al.* 2006; Thompson and Cohen 2006; Wu *et al.* 2008). The central role of the Hippo pathway as an integrator of other growth-related signals may also contribute to the abundance of tumor suppressors associated with Yki-driven growth (Harvey *et al.* 2013; Richardson and Portela 2017, 2018). Mis-regulation of this pathway also contributes to tumor formation in mouse models (Yu *et al.* 2015).

The potential of Yki/YAP expression to drive cellular transformation has been highlighted by studies of primary human cells in

regulators in the context of over expression of Yki. 228 of those formed a single cluster with PPI enrichment value 1.4E-06. Components of Fat/Hippo pathway (red: FDR-0.00076) and Autophagy genes (blue: FDR-0.0241) are enriched in this cluster. (C) STRING Interactome of 32 fly genes identified as potential oncogenes in the context of SOCS suppression. 27 out of those formed molecular clusters (with PPI enrichment value of 0.0122), largest being a cluster of 14 genes. A smaller cluster comprising of EGFR and DrK were enriched in Dorso-ventral axis formation (shown in purple: FDR-0.0089).
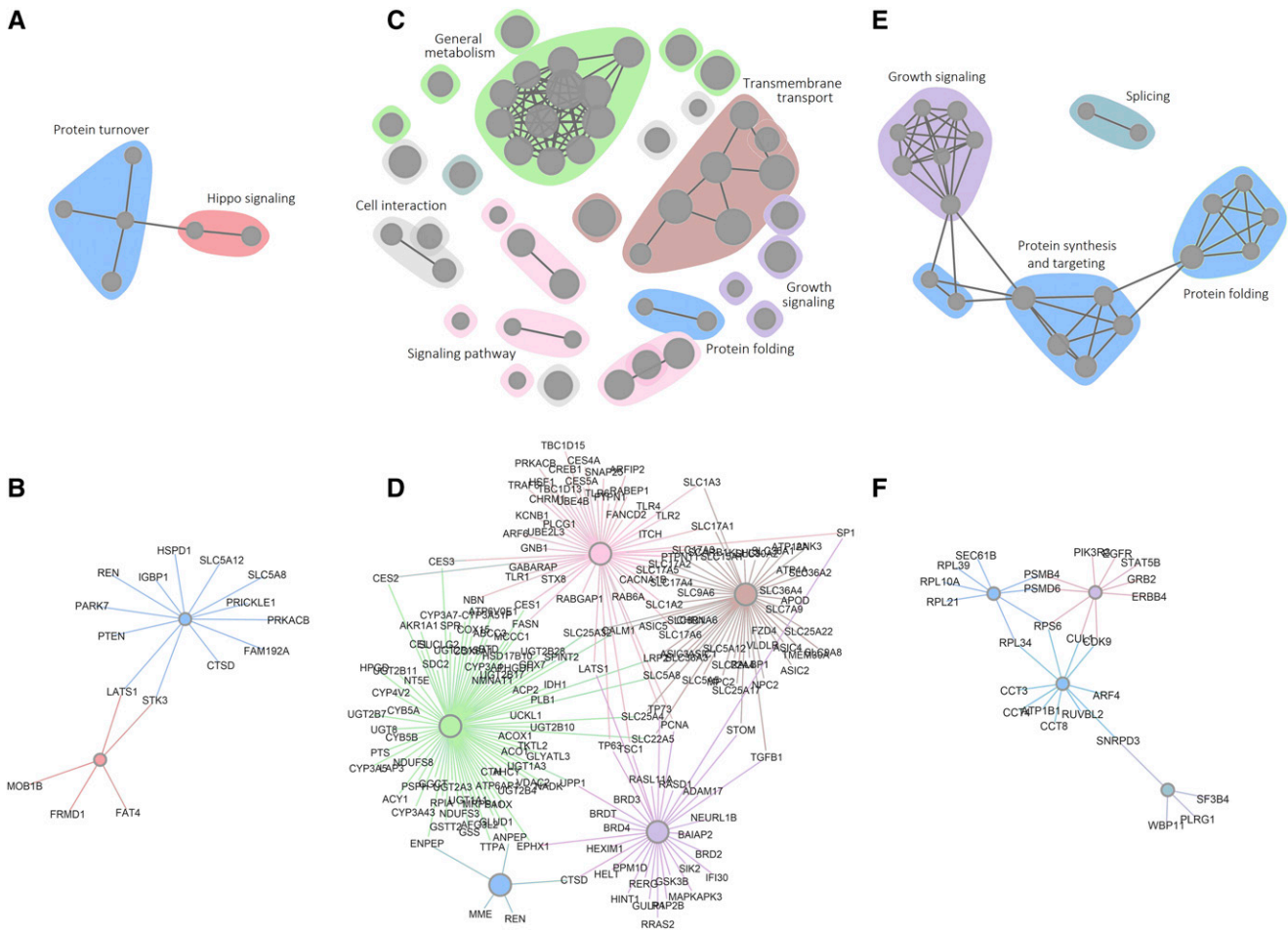
Figure 4 Summary of pathway enrichment analysis of human orthologs (A, C, E) The results of the pathway and gene set enrichment analysis are shown as enrichment maps. Each node represents a significantly enriched term or pathway from the GO, KEGG, Reactome and PANTHER, NCI, MsigDB, BIOCARTA databases (Table S3). Color-coding indicates functionally related groups of terms. Lines indicate genes shared among different terms. (B, D, F) show the individual genes associated with functionally enriched cluster. (A, B) UAS-EGFR screen (C, D) UAS-Yki screen (E, F) UAS-EGFR+UAS-SOCS36E[RNAi] screen.

culture, which have shown that YAP expression is both necessary and sufficient to confer a transformed phenotype involving anchorage independent growth and the ability to form tumors in xenograft models (Hong *et al.* 2014; Nguyen *et al.* 2014). We therefore consider it likely that the consequence of Yki overexpression predispose the tissue to transformation, allowing identification of a richer repertoire of cooperating factors. Indeed, YAP overexpression has been causally linked to formation of specific human tumors (Kapoor *et al.* 2014; Shao *et al.* 2014). The Hippo pathway has also been implicated in tumor formation resulting from cytokinesis failure (Ganem *et al.* 2014) and this has recently been linked to Yki-mediated regulation of string (CDC25) expression (Gerlach *et al.* 2018). The sensitivity of Yki-expressing tissue to tumor formation might be explained by the finding that Yki promotes cell cycle progression at both the G1-S transition (through regulation of cycE (Huang *et al.* 2005) and at the G2-M transition through regulation of string. In contrast, mitogens and growth factors such as EGFR typically induce growth by promoting G1-S, and therefore remain somewhat constrained by the G2-M checkpoint.

We have analyzed in more detail one group of genes, all related to regulating promoter proximal pausing of RNA Poly II, identified in this screen to validate the importance of the repertoire of genes

provided here. We have observed that Yki-driven growth is limited by the pausing of RNA Pol II, release of which is controlled by potential tumor suppressor genes (Nagarkar *et al.* 2020).

While our manuscript was in preparation, another group reported an RNAi screen to identify loci cooperating in tumorigenesis driven by expression in eye discs of the oncogenic activated mutant form of Ras (Zoranovic *et al.* 2018). We note that the activated Ras RNAi screen produced over 900 hits, compared with 74 for our EGFR screen, suggesting that the Ras screen was considerably more sensitized. We were surprised to note that there was almost no overlap between the two screens with only 3 hits in common: Elongin B, CG7966 and CG7313. This suggests that the genetic interactions required to promote tumorigenesis in the context of expression of an activated mutant form of RAS are distinct from those required to promote tumorigenesis in the context of native EGRF overexpression. And perhaps, the differences between the tissue contexts (eye discs in (Zoranovic *et al.* 2018) *vs.* wing discs in our screen). It will be of interest, in future, to learn whether this distinction holds true for factors promoting tumor formation in human cancers that depend on EGFR overexpression *vs.* those dependent on Ras mutants.

To conclude, the results reported here provide an extensive assessment of the genes that can serve as negative regulators of

growth that can contribute to the formation of neoplastic tumors *in vivo* in *Drosophila*. In addition to finding genes linked to known growth control pathways, a number of novel connections to Yki and EGFR driven tissue growth have been identified, which merit further investigation in the *Drosophila* genetic model. Exploring the potential relevance of genes identified in this manner to human cancer will involve assessing the correlation of candidate gene expression with clinical outcome across a broad range of cancers (*e.g.*, (Andrejeva *et al.* 2018; Eichenlaub *et al.* 2018)), as a starting point to identify biomarkers as well as novel candidate drug targets.

Note added in proof: See Nagarkar *et al.* 2020 (pp. 67–77) in *Genetics* 216:1 for a related work.

LITERATURE CITED

Alexandrov, L. B., S. Nik-Zainal, D. C. Wedge, S. A. J. R. Aparicio, S. Behjati *et al.*, 2013   Signatures of mutational processes in human cancer. Nature 500: 415–421. https://doi.org/10.1038/nature12477

Andrejeva, D., J. M. Kugler, H. T. Nguyen, A. Malmendal, M. L. Holm *et al.*, 2018   Metabolic control of PPAR activity by aldehyde dehydrogenase regulates invasive cell behavior and predicts survival in hepatocellular and renal clear cell carcinoma 11 Medical and Health Sciences 1112 Oncology and Carcinogenesis. BMC Cancer 18: 1–15.

Aragona, M., T. Panciera, A. Manfrin, S. Giulitti, F. Michielin *et al.*, 2013   A mechanical checkpoint controls multicellular growth through YAP/TAZ regulation by actin-processing factors. Cell 154: 1047–1059. https://doi.org/10.1016/j.cell.2013.07.042

Ashburner, M., C. A. Ball, J. A. Blake, D. Botstein, H. Butler *et al.*, 2000   Gene Ontology: tool for the unification of biology. Nat. Genet. 25: 25–29.

Brumby, A. M., K. R. Goulding, T. Schlosser, S. Loi, R. Galea *et al.*, 2011   Identification of novel Ras-cooperating oncogenes in Drosophila melanogaster: A RhoGEF/Rho-family/JNK pathway is a central driver of tumorigenesis. Genetics 188: 105–125. https://doi.org/10.1534/genetics.111.127910

Brumby, A. M., and H. E. Richardson, 2003   scribble mutants cooperate with oncogenic Ras or Notch to cause neoplastic overgrowth in Drosophila. EMBO J. 22: 5769–5779. https://doi.org/10.1093/emboj/cdg548

Cai, J., N. Zhang, Y. Zheng, R. F. De Wilde, A. Maitra *et al.*, 2010   The Hippo signaling pathway restricts the oncogenic potential of an intestinal re-generation program. Genes Dev. 24: 2383–2388. https://doi.org/10.1101/gad.1978810

Copeland, N. G., and N. A. Jenkins, 2010   Harnessing transposons for cancer gene discovery. Nat. Rev. Cancer 10: 696–706. https://doi.org/10.1038/nrc2916

Doggett, K., F. A. Grusche, H. E. Richardson, and A. M. Brumby, 2011   Loss of the Drosophila cell polarity regulator Scribbled promotes epithelial

tissue overgrowth and cooperation with oncogenic Ras-Raf through impaired Hippo pathway signaling. BMC Dev. Biol. 11: 57. https://doi.org/10.1186/1471-213X-11-57

Dong, J., G. Feldmann, J. Huang, S. Wu, N. Zhang *et al.*, 2007   Elucidation of a Universal Size-Control Mechanism in Drosophila and Mammals. Cell 130: 1120–1133. https://doi.org/10.1016/j.cell.2007.07.019

Eichenlaub, T., S. M. Cohen, and H. Herranz, 2016   Cell competition drives the formation of metastatic tumors in a drosophila model of epithelial tumor formation. Curr. Biol. 26: 419–427. https://doi.org/10.1016/j.cub.2015.12.042

Eichenlaub, T., R. Villadsen, F. C. P. Freitas, D. Andrejeva, B. I. Aldana *et al.*, 2018   Warburg Effect Metabolism Drives Neoplasia in a Drosophila Genetic Model of Epithelial Cancer. Curr. Biol. 28: 3220–3228.e6. https://doi.org/10.1016/j.cub.2018.08.035

Fabregat, A., S. Jupe, L. Matthews, K. Sidiropoulos, M. Gillespie *et al.*, 2018   The Reactome Pathway Knowledgebase. Nucleic Acids Res. 46: D649–D655. https://doi.org/10.1093/nar/gkx1132

Fanto, M., L. Clayton, J. Meredith, K. Hardiman, B. Charroux *et al.*, 2003   The tumor-suppressor and cell adhesion molecule fat controls planar polarity via physical interactions with Atrophin, a transcriptional co-repressor. Development 130: 763–774. https://doi.org/10.1242/dev.00304

Ganem, N. J., H. Cornils, S. Y. Chiu, K. P. O'Rourke, J. Arnaud *et al.*, 2014   Cytokinesis failure triggers hippo tumor suppressor pathway ac-tivation. Cell 158: 833–848. https://doi.org/10.1016/j.cell.2014.06.029

Gerlach, S. U., T. Eichenlaub, and H. Herranz, 2018   Yorkie and JNK Control Tumorigenesis in Drosophila Cells with Cytokinesis Failure. Cell Rep. 23: 1491–1503. https://doi.org/10.1016/j.celrep.2018.04.006

Gonzalez, C., 2013   Drosophila melanogaster: a model and a tool to in-vestigate malignancy and identify new therapeutics. Nat. Rev. Cancer 13: 172–183. https://doi.org/10.1038/nrc3461

Green, E. W., G. Fedele, F. Giorgini, and C. P. Kyriacou, 2014   A Drosophila RNAi collection is subject to dominant phenotypic effects. Nat. Methods 11: 222–223. https://doi.org/10.1038/nmeth.2856

Halder, G., S. Dupont, and S. Piccolo, 2012   Transduction of mechanical and cytoskeletal cues by YAP and TAZ. Nat. Rev. Mol. Cell Biol. 13: 591–600. https://doi.org/10.1038/nrm3416

Harvey, K. F., X. Zhang, and D. M. Thomas, 2013   The Hippo pathway and human cancer. Nat. Rev. Cancer 13: 246–257. https://doi.org/10.1038/nrc3458

Herranz, H., and S. M. Cohen, 2010   MicroRNAs and gene regulatory networks: Managing the impact of noise in biological systems. Genes Dev. 24: 1339–1344. https://doi.org/10.1101/gad.1937010

Herranz, H., T. Eichenlaub, and S. M. Cohen, 2016   Cancer in Drosophila: Imaginal Discs as a Model for Epithelial Tumor Formation. Curr. Top. Dev. Biol. 116: 181–199. https://doi.org/10.1016/bs.ctdb.2015.11.037

Herranz, H., X. Hong, and S. M. Cohen, 2012a   Mutual repression by bantam miRNA and capicua links the EGFR/MAPK and hippo pathways in growth control. Curr. Biol. 22: 651–657. https://doi.org/10.1016/j.cub.2012.02.050

Herranz, H., X. Hong, N. T. Hung, P. Mathijs Voorhoeve, and S. M. Cohen, 2012b   Oncogenic cooperation between SOCS family proteins and EGFR identified using a Drosophila epithelial transformation model. Genes Dev. 26: 1602–1611. https://doi.org/10.1101/gad.192021.112

Herranz, H., R. Weng, and S. M. Cohen, 2014   Crosstalk between epithelial and mesenchymal tissues in tumorigenesis and imaginal disc development. Curr. Biol. 24: 1476–1484. https://doi.org/10.1016/j.cub.2014.05.043

Hong, X., H. T. Nguyen, Q. Chen, R. Zhang, Z. Hagman *et al.*, 2014   Opposing activities of the R as and H ippo pathways converge on regulation of YAP protein turnover. EMBO J. 33: 2447–2457. https://doi.org/10.15252/embj.201489385

Huang, J., S. Wu, J. Barrera, K. Matthews, and D. Pan, 2005   The Hippo signaling pathway coordinately regulates cell proliferation and apoptosis by inactivating Yorkie, the Drosophila homolog of YAP. Cell 122: 421–434. https://doi.org/10.1016/j.cell.2005.06.007

Kandoth, C., M. D. McLellan, F. Vandin, K. Ye, B. Niu *et al.*, 2013   Mutational landscape and significance across 12 major cancer types. Nature 502: 333–339. https://doi.org/10.1038/nature12634

Kanehisa, M., M. Furumichi, M. Tanabe, Y. Sato, and K. Morishima, 2017   KEGG: New perspectives on genomes, pathways, diseases and drugs. Nucleic Acids Res. 45: D353–D361. https://doi.org/10.1093/nar/gkw1092

Kanehisa, M., Y. Sato, M. Kawashima, M. Furumichi, and M. Tanabe, 2016   KEGG as a reference resource for gene and protein annotation. Nucleic Acids Res. 44: D457–D462. https://doi.org/10.1093/nar/gkv1070

Kapoor, A., W. Yao, H. Ying, S. Hua, A. Liewen et al., 2014   Yap1 activation enables bypass of oncogenic KRAS addiction in pancreatic cancer. Cell 158: 185–197. https://doi.org/10.1016/j.cell.2014.06.003

McGranahan, N., and C. Swanton, 2017   Clonal Heterogeneity and Tumor Evolution: Past, Present, and the Future. Cell 168: 613–628. https://doi.org/10.1016/j.cell.2017.01.018

Menut, L., T. Vaccari, H. Dionne, J. Hill, G. Wu et al., 2007   A mosaic genetic screen for Drosophila neoplastic tumor suppressor genes based on defective pupation. Genetics 177: 1667–1677. https://doi.org/10.1534/genetics.107.078360

Nagarkar, S., R. Wasnik, P. Govada, S. M. Cohen, and L. S. Shashidhara, 2020   Promoter proximal pausing limits Yki-induced tumorous growth in Drosophila. Genetics. https://doi.org/10.1534/genetics.120.303419.

Nguyen, H. T., X. Hong, S. Tan, Q. Chen, L. Chan et al., 2014   Viral small T oncoproteins transform cells by alleviating Hippo-pathway-mediated inhibition of the YAP proto-oncogene. Cell Rep. 8: 707–713. https://doi.org/10.1016/j.celrep.2014.06.062

Nolo, R., C. M. Morrison, C. Tao, X. Zhang, and G. Halder, 2006   The bantam MicroRNA Is a Target of the Hippo Tumor-Suppressor Pathway. Curr. Biol. 16: 1895–1904. https://doi.org/10.1016/j.cub.2006.08.057

Pagliarini, R. A., and T. Xu, 2003   A genetic screen in Drosophila for metastatic behavior. Science 302: 1227–1231. https://doi.org/10.1126/science.1088474

Pereira, B., S.-F. Chin, O. M. Rueda, H.-K. M. Vollan, E. Provenzano et al., 2016   The somatic mutation profiles of 2,433 breast cancers refine their genomic and transcriptomic landscapes. Nat. Commun. 7: 11479.

Pérez-Mancera, P. A., A. G. Rust, L. Van Der Weyden, G. Kristiansen, A. Li et al., 2012   The deubiquitinase USP9X suppresses pancreatic ductal adenocarcinoma. Nature 486: 266–270. https://doi.org/10.1038/nature11114

Reddy, B. V. V. G., and K. D. Irvine, 2013   Regulation of Hippo Signaling by EGFR-MAPK Signaling through Ajuba Family Proteins. Dev. Cell 24: 459–471. https://doi.org/10.1016/j.devcel.2013.01.020

Ren, F., L. Zhang, and J. Jiang, 2010   Hippo signaling regulates Yorkie nuclear localization and activity through 14–3–3 dependent and independent mechanisms. Dev. Biol. 337: 303–312. https://doi.org/10.1016/j.ydbio.2009.10.046

Richardson, H. E., and M. Portela, 2018   Modelling Cooperative Tumorigenesis in Drosophila. BioMed Res. Int. 2018: 4258387. https://doi.org/10.1155/2018/4258387

Richardson, H. E., and M. Portela, 2017   Tissue growth and tumorigenesis in Drosophila: cell polarity and the Hippo pathway. Curr. Opin. Cell Biol. 48: 1–9. https://doi.org/10.1016/j.ceb.2017.03.006

Shao, D. D., W. Xue, E. B. Krall, A. Bhutkar, F. Piccioni et al., 2014   KRAS and YAP1 converge to regulate EMT and tumor survival. Cell 158: 171–184. https://doi.org/10.1016/j.cell.2014.06.004

Song, S., H. Herranz, and S. M. Cohen, 2017   The chromatin remodeling BAP complex limits tumor-promoting activity of the Hippo pathway effector Yki to prevent neoplastic transformation in Drosophila epithelia. DMM Dis. Model. Mech. 10: 1201–1209. https://doi.org/10.1242/dmm.030122

Sonoshita, M., and R. L. Cagan, 2017   Modeling Human Cancers in Drosophila, Elsevier Inc., Amsterdam. https://doi.org/10.1016/bs.ctdb.2016.07.008

Stratton, M. R., 2011   Exploring the genomes of cancer cells: progress and promise. Science 331: 1553–1558. https://doi.org/10.1126/science.1204040

Szklarczyk, D., J. H. Morris, H. Cook, M. Kuhn, S. Wyder et al., 2017   The STRING database in 2017: Quality-controlled protein-protein association networks, made broadly accessible. Nucleic Acids Res. 45: D362–D368. https://doi.org/10.1093/nar/gkw937

Takeda, H., Z. Wei, H. Koso, A. G. Rust, C. C. K. Yew et al., 2015   Transposon mutagenesis identifies genes and evolutionary forces driving gastrointestinal tract tumor progression. Nat. Genet. 47: 142–150. https://doi.org/10.1038/ng.3175

Tapon, N., K. F. Harvey, D. W. Bell, D. C. R. Wahrer, T. A. Schiripo et al., 2002   salvador promotes both cell cycle exit and apoptosis in Drosophila and is mutated in human cancer cell lines. Cell 110: 467–478. https://doi.org/10.1016/S0092-8674(02)00824-3

Thomas, P. D., M. J. Campbell, A. Kejariwal, H. Mi, B. Karlak et al., 2003   PANTHER: A library of protein families and subfamilies indexed by function. Genome Res. 13: 2129–2141. https://doi.org/10.1101/gr.772403

Thompson, B. J., and S. M. Cohen, 2006   The Hippo Pathway Regulates the bantam microRNA to Control Cell Proliferation and Apoptosis in Drosophila. Cell 126: 767–774. https://doi.org/10.1016/j.cell.2006.07.013

Vissers, J. H. A., S. A. Manning, A. Kulkarni, and K. F. Harvey, 2016   A Drosophila RNAi library modulates Hippo pathway-dependent tissue growth. Nat. Commun. 7: 10368. https://doi.org/10.1038/ncomms10368

Wada, K. I., K. Itoga, T. Okano, S. Yonemura, and H. Sasaki, 2011   Hippo pathway regulation by cell morphology and stress fibers. Development 138: 3907–3914. https://doi.org/10.1242/dev.070987

Willecke, M., J. Toggweiler, and K. Basler, 2011   Loss of PI3K blocks cell-cycle progression in a Drosophila tumor model. Oncogene 30: 4067–4074. https://doi.org/10.1038/onc.2011.125

Willoughby, L. F., T. Schlosser, S. A. Manning, J. P. Parisot, I. P. Street et al., 2013   An in vivo large-scale chemical screening platform using Drosophila for anti-cancer drug discovery. DMM Dis. Model. Mech. 6: 521–529. https://doi.org/10.1242/dmm.009985

Wu, S., Y. Liu, Y. Zheng, J. Dong, and D. Pan, 2008   The TEAD/TEF family protein Scalloped mediates transcriptional output of the Hippo growth-regulatory pathway. Dev. Cell 14: 388–398. https://doi.org/10.1016/j.devcel.2008.01.007

Wu, M., J. C. Pastor-Pareja, and T. Xu, 2010   Interaction between Ras(V12) and scribbled clones induces tumour growth and invasion. Nature 463: 545–548. https://doi.org/10.1038/nature08702

Yu, G., and Q. Y. He, 2016   ReactomePA: An R/Bioconductor package for reactome pathway analysis and visualization. Mol. Biosyst. 12: 477–479. https://doi.org/10.1039/C5MB00663E

Yu, G., L. G. Wang, Y. Han, and Q. Y. He, 2012   ClusterProfiler: An R package for comparing biological themes among gene clusters. Omi. A J. Integr. Biol. 16: 284–287.

Yu, F. X., B. Zhao, and K. L. Guan, 2015   Hippo Pathway in Organ Size Control, Tissue Homeostasis, and Cancer. Cell 163: 811–828. https://doi.org/10.1016/j.cell.2015.10.044

Zehir, A., R. Benayed, R. H. Shah, A. Syed, S. Middha et al., 2017   Mutational landscape of metastatic cancer revealed from prospective clinical sequencing of 10,000 patients. Nat. Med. 23: 703–713. https://doi.org/10.1038/nm.4333

Zoranovic, T., J. Manent, L. Willoughby, R. Matos de Simoes, J. E. La Marca et al., 2018   A genome-wide Drosophila epithelial tumorigenesis screen identifies Tetraspanin 29Fb as an evolutionarily conserved suppressor of Ras-driven cancer. PLoS Genet. 14: e1007688. https://doi.org/10.1371/journal.pgen.1007688

Communicating editor: B. Andrews